TELKOMNIKA Telecommunication Computing Electronics and Control
Vol. 24, No. 2, April 2026, pp. 407~419
ISSN: 1693-6930, DOI: 10.12928/TELKOMNIKA.v24i2.27396

Noise-suppression method for UAV-OFDM systems by introducing CV-VSS-NLMS algorithm and single-antenna architecture

Walid Lebbou[1], Laid Chergui[1], Saad Bouguezel[2]
[1]Laboratory of Satit, Department of Electrical Engineering, Université Abbes Laghrour Khenchela, Khenchela, Algeria
[2]CCNS Laboratory, Department of Electronics, Setif 1 University Ferhat Abbas, Sétif, Algeria

Article Info

Article history:

Received Jul 13, 2025
Revised Dec 8, 2025
Accepted Jan 30, 2026

Keywords:

Least mean square algorithm
Noise cancellation
Orthogonal frequency division multiplexing
Unmanned aerial vehicle
Wireless communication

ABSTRACT

In this paper, we address the critical challenge of impulsive interference in orthogonal frequency division multiplexing (OFDM)-based unmanned aerial vehicle (UAV) communication systems, which can severely degrade data transmission reliability. Specifically, we propose a novel complex-valued variable step-size normalized least mean square (CV-VSS-NLMS) adaptive filtering algorithm dedicated for adaptive filtering of complex-valued signals, providing real-time, lightweight, and efficient impulsive-noise suppression for UAV-OFDM signals. In contrast, real-valued VSS-LMS filters treat the real and imaginary parts separately, resulting in poorer mean square error (MSE) convergence for complex signals. The algorithm is developed by efficiently adapting LMS-based filtering strategies to impulsive interference scenarios and adequately integrating prior concepts of electromagnetic pulse suppression within a well-designed single-antenna UAV architecture. This new configuration is especially suited for size, weight, and power-constrained UAV platforms, where reducing complexity is highly desirable. In contrast to conventional blind source separation approaches, the proposed solution ensures reliable communication without excessive processing demands, since it efficiently suppresses impulsive noise and greatly reduces the number of matrix operations. Simulation results demonstrate a significant improvement in bit error rate (BER), confirming that the proposed CV-VSS-NLMS technique provides a robust, dependable, and practical solution for modern UAV communication links.

Corresponding Author:

Laid Chergui
Laboratory of Satit, Department of Electrical Engineering, Université Abbes Laghrour Khenchela
Khenchela, 40004, Algeria
Email: chergui_laid@univ-khenchela.dz

1. INTRODUCTION

In recent years, unmanned aerial vehicles (UAVs) have gained considerable importance, highlighting their essential role in daily life. They have emerged as crucial solutions in various fields, including research, medicine, industry, environmental monitoring, communication technologies and security [1]-[5].

Among the communication techniques used in UAVs, the orthogonal frequency division multiplexing (OFDM) is widely adopted for its high transmission speed, good spectral efficiency, and ability to mitigate inter-symbol interference (ISI) and inter-carrier interference (ICI) [6]-[13]. However, the OFDM in UAVs is susceptible to impulsive interference from sources like switching processes in power networks, ignition noise from passing vehicles, and other systems operating in the same frequency range [14]-[16]. Moreover, OFDM systems can tolerate moderate and infrequent impulsive interference fairly well, as this

interference is spread across multiple sub-carriers of an OFDM symbol. However, when interference occurs frequently or has high power, it significantly impacts system performance [17], [18] necessitating the use of interference mitigation techniques [19], [20].

In the literature, research has focused on analyzing noise in wireless communication links using single electromagnetic pulses like gaussian and square wave pulses [21]-[26]. The information security of UAV communication links in complex electromagnetic environments was first addressed in [27], where analytical functions have been established for typical noise, such as high-voltage sinusoidal pulses (HVSP), electrical fast transient pulses (EFTP), and surge pulses (SP).

It should be noted that [27] was the first to consider the integration of UAV modulation and demodulation methods, based on the principles of OFDM, with electromagnetic pulse interference and its suppression. This approach, which is a source separation technique that incorporates a dual antenna design alongside OFDM-based noise suppression techniques, has demonstrated strong performance in mitigating electromagnetic noise in UAV communications, leading to enhanced image quality and reduced bit error rate (BER). However, this approach is computationally intensive, primarily due to the calculation of the covariance matrix required during the whitening phase. This whitening process, which removes correlations between observed signals, precedes the iterative separation of the useful signal from electromagnetic noise and simplifies the extraction of independent components. While whitening significantly improves the convergence of the algorithm, it also contributes substantially to the overall computational complexity of the technique. Consequently, this method is not well suited for real-time applications, as it operates on data blocks rather than processing signals continuously.

There are also several source separation techniques in the literature, such as the least mean square (LMS)-based symmetric adaptive decorrelation (SAD) algorithm discussed in [28], which distinguishes between signal and noise to enable effective signal separation. Additionally, recent advancements include the proposal of two-channel variable-step-size forward-and-backward adaptive algorithm structures for speech enhancement in scenarios involving highly correlated noisy observations [29].

In this paper, we propose a novel approach for mitigating impulsive interference in UAV OFDM communication systems. The core contribution of this approach lies in the introduction of a complex-valued variable step size normalized LMS (CV-VSS-NLMS) algorithm, which is exclusively developed for real-time sample-by-sample noise cancellation and dedicated for adaptive filtering of complex-valued signals. In contrast, the existing real valued VSS-LMS algorithms must filter the real and imaginary parts separately, resulting in poorer mean square error (MSE) convergence. The proposed approach adapts existing LMS-based adaptive filtering principles and integrates concepts from prior electromagnetic pulse suppression techniques. In order to achieve efficient, lightweight, and real-time noise suppression in UAV-OFDM communication systems, we introduce a combination of the proposed CV-VSS-NLMS algorithm and a well-designed single-antenna architecture. Unlike conventional blind source separation methods that rely on multiple matrix computations and block processing, the proposed combination approach significantly reduces the computational complexity while maintaining high performance.

The remainder of this paper is organized as follows: section 2 describes in detail the proposed methodology. Section 3 presents and discusses the simulation results. Finally, section 4 concludes the paper and summarizes the main findings, as well as possible directions for future work.

2. METHODOLOGY

2.1. Review of electromagnetic pulse suppression method for OFDM-based UAV

In this sub-section, we present a review of the dual-antenna pulse noise mitigation technique reported in [27], which corresponds to the electromagnetic pulse suppression method for OFDM-based UAV communication. This method is illustrated in Figures 1 and 2, which show that the process involves several stages, including demeaning, combination, whitening, iterative operations, and convergence assessment.

It is seen from Figure 2 that the two signals $x^1 = [x_0^1, x_1^1, \ldots, x_{K-1}^1]^T$ and $x^2 = [x_0^2, x_1^2, \ldots, x_{K-1}^2]^T$, where K is the number of samples and $[\cdot]^T$ denotes the matrix transpose operation, are captured by two separated antennas and then passed through a de-mean module. This module subtracts the mean value of a given signal from each of its samples, resulting in the new signals $\bar{x}^1 = [\bar{x}_0^1, \bar{x}_1^1, \ldots, \bar{x}_{K-1}^1]^T$ and $\bar{x}^2 = [\bar{x}_0^2, \bar{x}_1^2, \ldots, \bar{x}_{K-1}^2]^T$ whose samples are computed as:

$$\bar{x}_n^i = x_n^i - \frac{1}{K}\sum_{k=0}^{K-1} x_k^i,\ i = 1, 2 \text{ and } n = 0, 1, 2, \ldots, K\text{-}1 \quad (1)$$

The purpose of the de-mean carried out in (1) is to enhance the convergence of the iterative computation process. The two signals resulted from (1) are then combined in a single signal in the form of a two-row matrix as:

$$X = \begin{bmatrix} (\bar{x}^1)^T \\ (\bar{x}^2)^T \end{bmatrix} \quad (2)$$

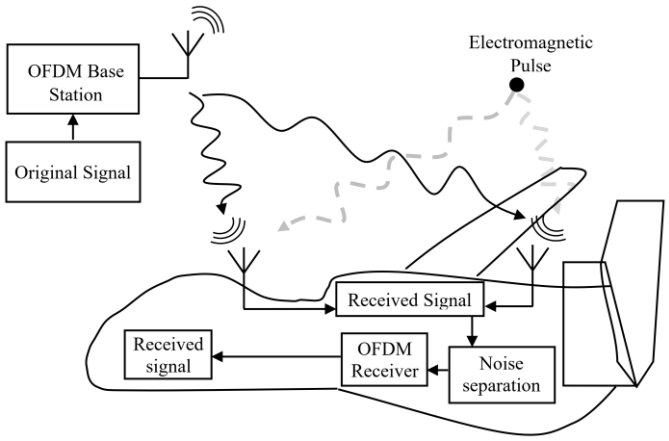

Figure 1. Schematic diagram of the uplink transmission link for UAV [27]

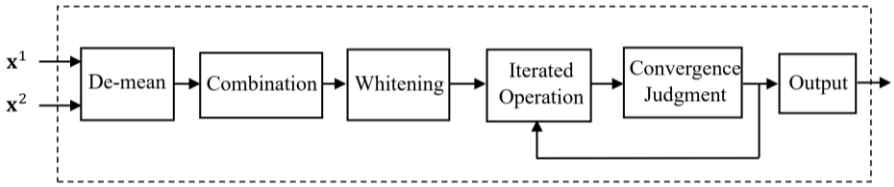

Figure 2. Schematic diagram of separation module of electromagnetic pulse noise from OFDM wireless signal [27]

The process of whitening of the signal X resulted in (2) is performed as:

$$Z = \Lambda^{-\frac{1}{2}} u^T X \quad (3)$$

Where u and Λ are respectively the eigenvector and eigenvalue matrixes of the covariance matrix C_X given by:

$$C_x = \left(\frac{1}{M}\right) X^T X \quad (4)$$

where M corresponds to the number of the captured signals, which is considered to be equal to 2.

The matrix Z whitened in (3), which can be expressed as $Z = [z1\ z2]$, is subsequently utilized in the iterative computation process performed for each weight vector as:

$$w1^i = E\{z^i * tanh(W^T \times Z)\} - E\{1 - (tanh(W^T \times Z)^2)\} * w^i,\ i = 1, 2 \quad (5)$$

where $w^i = [w_0^i, w_1^i, \ldots, w_{M-1}^i]^T$, $i = 1, 2$, are two weight vectors used during the iterative process, which are combined in a two-row matrix as $W = [w^1 \quad w^2]$, the operators × and * denote, respectively, the dot and Hadamard products, and $E\{\cdot\}$ is the expectation operation. The two vectors $w1^i = [w1_0^i, w1_1^i, \ldots, w1_{M-1}^i]^T$, $i = 1, 2$, resulted from (5) are also arranged in a two-row matrix as $W1 = [w1^1 \quad w1^2]$.

By adapting the vector $W1$, a new vector $W2$is obtained as:

$$W2 = W1 - \sum_{i=1}^{M-1} [W1^T \times w^i] * w^i \quad (6)$$

which can be expressed as $W2 = [w2^1 \quad w2^2]$, where $w2^i = [w2_0^i, w2_1^i, \ldots, w2_{M-1}^i]^T$, i=1, 2. These two weight vectors are normalized as:

$$\widetilde{w}^i = w2^i / \|w2^i\|, i = 1, 2 \tag{7}$$

and then combined in a two-row matrix as $\widetilde{W} = [\widetilde{w}^1 \quad \widetilde{w}^2]$, where $\|\cdot\|$ denotes the norm operation defined as:

$$\|w2^i\| = \sqrt{\sum_{k=0}^{M-1} \left(w2_k^i\right)^2}, i = 1, 2. \text{ and } M = 2 \tag{8}$$

In the iterative process, $W1$ and $W2$ are intermediate variables matrixes derived from W. The matrix $\widetilde{W}$ represents the update of W after each iteration.

After each iteration, the condition given by:

$$|\widetilde{W} + W| < q \tag{9}$$

must be verified, where q is the convergence value used to judge the convergence of $\widetilde{W}$.

If condition (9) is satisfied, W is considered to have converged. Otherwise, $\widetilde{W}$ is updated and used as the new W according to:

$$\widetilde{W} = W \tag{10}$$

Finally, the output demixing matrix is then obtained as:

$$S = \widetilde{W}^T Z \tag{11}$$

The matrix S, derived using $\widetilde{W}$, contains both noise and the original signal. This process ensures that the hybrid matrix Z achieves maximum non-Gaussianity, allowing for effective component separation and facilitating the extraction of the signal of interest from S.

2.2. Proposed approach

In this sub-section, we present a novel noise mitigation system for the UAV communication link by using three adaptive noise cancellers (ANCs) units and introducing a new CV-VSS-NLMS algorithm. These three cancellers operate in parallel, each using one of the three types of noise as a reference input signal to give an estimation $\hat{n}_k$ of the unknown complex valued noise n_k present in the captured signal given as:

$$d_k = s_k + n_k \tag{12}$$

The complex valued reference signals are specifically defined as follows: ${x_k}^{(1)} = {n_k}^{(1)}$, ${x_k}^{(2)} = {n_k}^{(2)}$ and ${x_k}^{(3)} = {n_k}^{(3)}$. The estimated noises are then subtracted from d_k to de-noise the desired signal of interest s_k.

At the output of the proposed system, we designed a module using a cost function to identify which of the three ANC's provides the best de-noised version $\hat{s}_k$ of the desired signal s_k. Each of the three CV-VSS-NLMS ANCs is defined by:

$${w_{k+1}}^{(i)} = w_k^{(i)} + {\mu_k}^{(i)} {\hat{s}_k}^{(i)} \frac{\left(x_k^{(i)}\right)^*}{\left(x_k^{(i)}\right)^H x_k^{(i)} + \varepsilon}, i = 1, 2, 3 \tag{13}$$

where $(\cdot)^*$ and $(\cdot)^H$ denote the complex conjugate and the Hermitian transpose operations, respectively. ${w_k}^{(i)} = \left[w_k^{(i)}(0), w_k^{(i)}(1), \ldots, w_k^{(i)}(N-1)\right]^T$ is the filter weight vector of length N, i =1, 2,3 and the term $\left(x_k^{(i)}\right)^H x_k^{(i)}$ corresponds to the power estimate of $x_k^{(i)}$, which enables its power normalization, the parameter ε is a regularization term that takes small values to prevent overflow, and ${\mu_k}^{(i)}$ is the variable step-size parameter used to control the convergence behavior of the adaptive algorithm. The input signals $x_k^{(i)}$, i = 1, 2, 3, of the adaptive filters correspond to the three considered noise types. Specifically, the noise types are ${n_k}^{(1)}$: HVSP, ${n_k}^{(2)}$: EFTP, and ${n_k}^{(3)}$: SP.

The estimated signal at the output of each of the three ANCs is then computed as:

$$\hat{s}_k^{(i)} = d_k - \left(w_k^{(i)}\right)^T x_k^{(i)} \tag{14}$$

where $(\cdot)^T$ denote the transpose operation, whereas the variable step size $\mu_k{}^{(i)}$ in (13) is defined as:

$$\mu_k{}^{(i)} = \alpha \mu_{k-1}{}^{(i)} + \gamma \left\| \hat{p}_k{}^{(i)} \right\|^2 \tag{15}$$

where,

$$\hat{p}_k{}^{(i)} = \delta \hat{p}_{k-1}{}^{(i)} + (1-\delta)\hat{s}_k{}^{(i)} \frac{\left(x_k^{(i)}\right)^*}{\left(x_k^{(i)}\right)^H x_k^{(i)} + \varepsilon} \tag{16}$$

the parameters α and $\gamma$are positive scalars used for controlling the variable step size $\mu_k{}^{(i)}$, and δ is the smoothing factor with values taken in the range (0, 1).

It should be noted that the proposed CV-VSS-NLMS algorithm formulated in (13)-(16) is derived from the variable step size pre-whitening transform-domain LMS introduced in [30] for an ANC system operating in the transform domain. However, in the present work, the proposed CV-VSS-NLMS-based ANC algorithm operates in the time domain.

In contrast to the system in [27], the proposed system requires only a single antenna as shown in Figure 3, and the interfering noise n_k in (12), affecting the UAV communication link, can be one of the three considered types of noise.

To identify which of the outputs $\hat{s}_k{}^{(i)}$, i = 1, 2, 3, corresponds to the best de-noised recovered signal, we have designed an identification system based on the calculation of a cost function. This system relies on the estimation of the average energy of the signal$\hat{s}_k{}^{(i)}$, recovered at the output of each ANC, in order to determine the type of noise that contaminated the received signal.

The average energy is computed, at each instant *k*, after the convergence of the CV-VSS-NLMS algorithms, as [31]:

$$\begin{cases} E_k{}^{(i)} = \frac{1}{L}\sum_{n=0}^{L-1} \hat{s}_{k-n}{}^{(i)} \times \left(\hat{s}_{k-n}{}^{(i)}\right)^* & \text{if} \quad k \geq n \\ 0 & \text{otherwise} \end{cases} \tag{17}$$

where *L* is the length of the smoothing window.

Subsequently, we look for the lowest average energy among $E_k{}^{(1)}$, $E_k{}^{(2)}$ and$E_k{}^{(3)}$, and consequently, the corresponding estimated signal is considered to be the one at the output of the system. The proposed system replaces the existing separation module in the OFDM-Based UAV receiver with a module that uses only a single antenna as the signal source.

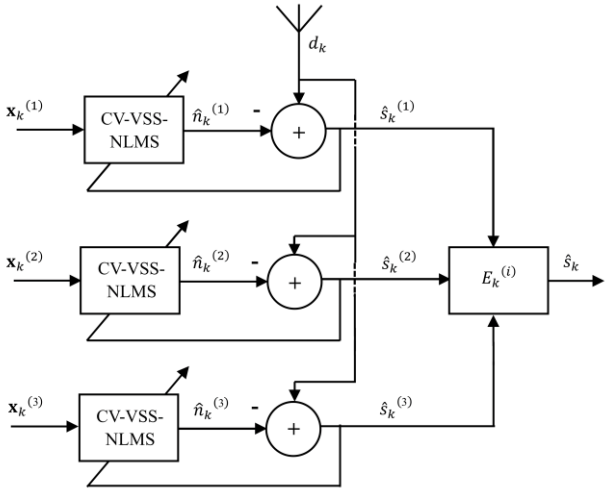

Figure 3. Proposed system

3. RESULTS AND DISCUSSIONS

3.1. Simulations

In this section, we simulate the proposed system under the same conditions considered in [27]. We use the three considered noises, namely: HVSP, the EFTP and the SP. The field analytic functions of the noises are defined respectively by (18)-(20) as:

$$EF^{(1)}(t) = c\,sin(\,2\pi f_D t + \varphi) \tag{18}$$

where c = 500 V/m, f_D = 4 kHz and φ = +0 rad. This noise is a strong electromagnetic pulse generated near high-voltage transmission lines, which significantly impacts drone communication link [32].

$$EF^{2}(t) = \begin{cases} t \times 10^{9}, 0 \le t \le 4.4 \cdot 10^{-9} \\ 4.4e^{-0.11\times(t-4.4\times10^{9})\times10^{9}}, 4.4 \cdot 10^{-9} \le t \le 1000 \times 10^{-9} \end{cases} \tag{19}$$

$$EF^{3}(t) = \begin{cases} e^{0.48\times10^{12}\times t^{2}} - 1 \quad, 0 \le t \le 1.2 \times 10^{-6} \\ -t - 1.2 \times 10^{-6} \times 10^{4} + 1, 1.2 \times 10^{-6} \le t \le 130 \times 10^{-6} \\ t - 1.2 \times 10^{-6} \times 10^{4} - 0.570, 130 \times 10^{6} \le t \le 158 \times 10^{-6} \end{cases} \tag{20}$$

These pulse noises continuously disrupt wireless communication with their instantaneous energy being sufficient to directly cause drone communication failures [27], [33], [34]. The single pulse waveforms of the three noises are presented in Figures 4(a) to (c).

The baud rate for a fixed-wing UAV is typically assumed to be 4000, while the carrier frequency f_c is set to 4 kHz. These parameters commonly adopted as standard simulation conditions to comprehensively analyze the impact of various electromagnetic pulses on the communication link, ensuring the results remain broadly applicable, see Table 1.

The OFDM transceiver employs a quadrature phase shift keyin (QPSK) modulation scheme with an fast fourier transform (FFT) size of 32 and a cyclic prefix length of 8. The parameters of the CV-VSS-NLMS adaptive filters used for all ANCs are listed in Table 2. To assess the system's capability to identify the type of noise affecting the UAV communication link, i.e., the interference impacting the signal of interest in (12), and to evaluate its denoising performance, several key criteria are considered. These include the residual noise energy in the denoised signal, the convergence behavior of the MSE for the CV-VSS-NLMS algorithms, and the BER of the received signal.

To simulate realistic flight conditions, a Rayleigh fading channel with Doppler effects is adopted. The channel model consists of 10 coefficients, corresponding to a UAV velocity of 20 m/s, a carrier frequency of 5 GHz, and a resulting Doppler frequency of 333.33 Hz. The channel bandwidth is set to 10 MHz. The OFDM system parameters in this case include a 64-point FFT and a cyclic prefix length of 12 [35].

At the receiver side, the resulting signal d_k in (12) becomes:

$$d_k = s_k * h + n_k \tag{21}$$

where $(*)$denotes the convolution operation, and h denotes the impulse response of the Rayleigh fading channel with Doppler effects. The key performance criterion considered in this study is the convergence behavior of the MSE.

To achieve this, we conducted three distinct experiments, each focusing on a specific type of noise: $n_k^{(1)}$, $n_k^{(2)}$ and $n_k^{(3)}$ as defined in (18)-(20), respectively.

Table I. Simulation parameters [27]

Parameters	Values
Baud rate (for a fixed-wing UAV)	4000
Sampling frequency f_s of the receiving end	64 kHz
Low-pass filter cut-off frequency f_w	6 kHz
Electric field strength generated by the communication link	5 V/m
Electric field strength generated by the pulse signal	500 V/m
Carrier Frequency f_c	4 kHz

Table 2. CV-VSS-NLMS algorithm parameters

Parameters	Values
Filter length N	8
Initial $\mu_k{}^{(1)}$	0.9
Initial $\mu_k{}^{(2)}$	0.1
Initial $\mu_k{}^{(3)}$	1.2
α	0.999
γ	0.00005
δ	0.99
ε	0.1

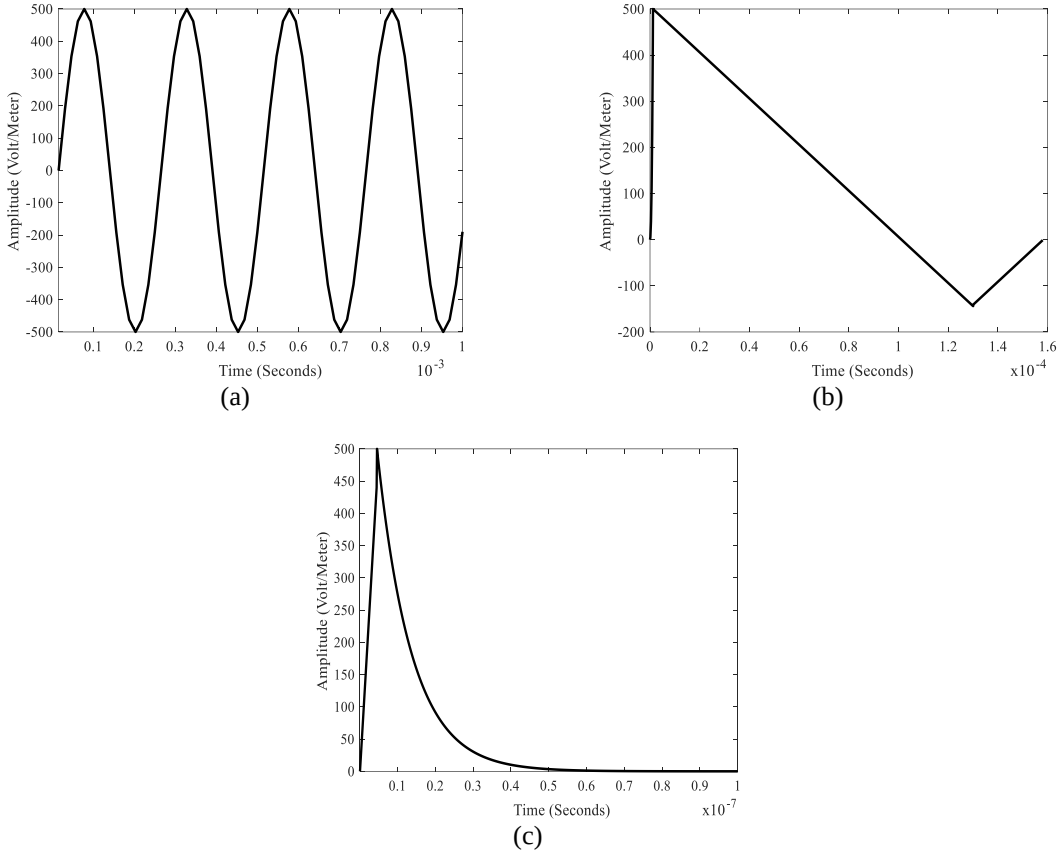

Figure 4. Representative waveforms of the three considered high-voltage interference noises: (a) high-voltage sinusoidal pulse waveform, (b) single high voltage EFTP pulse waveform, and (c) single high voltage surge pulse waveform

These experiments were carried out to rigorously evaluate the performance of the system across diverse conditions and to confirm its robustness in handling different types of noise. In each experiment, the average energies $E_k{}^{(i)}$, as defined in (17), are computed. Figures 5(a) to (d) depict the convergence behavior of the MSE for the three ANCs in the proposed system, evaluated under communication links individually affected by three distinct types of noise: HVSP, EFTP, and SP, respectively.

The results obtained for both channel conditions, namely, the flat fading channel and the UAV Rayleigh Doppler channel, clearly indicate that each adaptive filter, when driven by a specific noise source, performs effectively when the communication link is subject to the same type of disturbance. This effectiveness is more pronounced under the flat fading channel, where the filters exhibit superior MSE convergence performance, characterized by a faster convergence rate and a lower steady-state level. This behavior reflects the efficiency of the adaptation mechanism, demonstrating the capability of the CV-VSS-NLMS filters to selectively suppress the noise type for which they were originally designed. In contrast, under the UAV Rayleigh Doppler scenario, a degradation in the steady-state MSE is observed. This degradation is attributed to the Doppler-induced time variations of the channel, which alter the statistical properties of the received signal and consequently deteriorate the convergence performance [36].

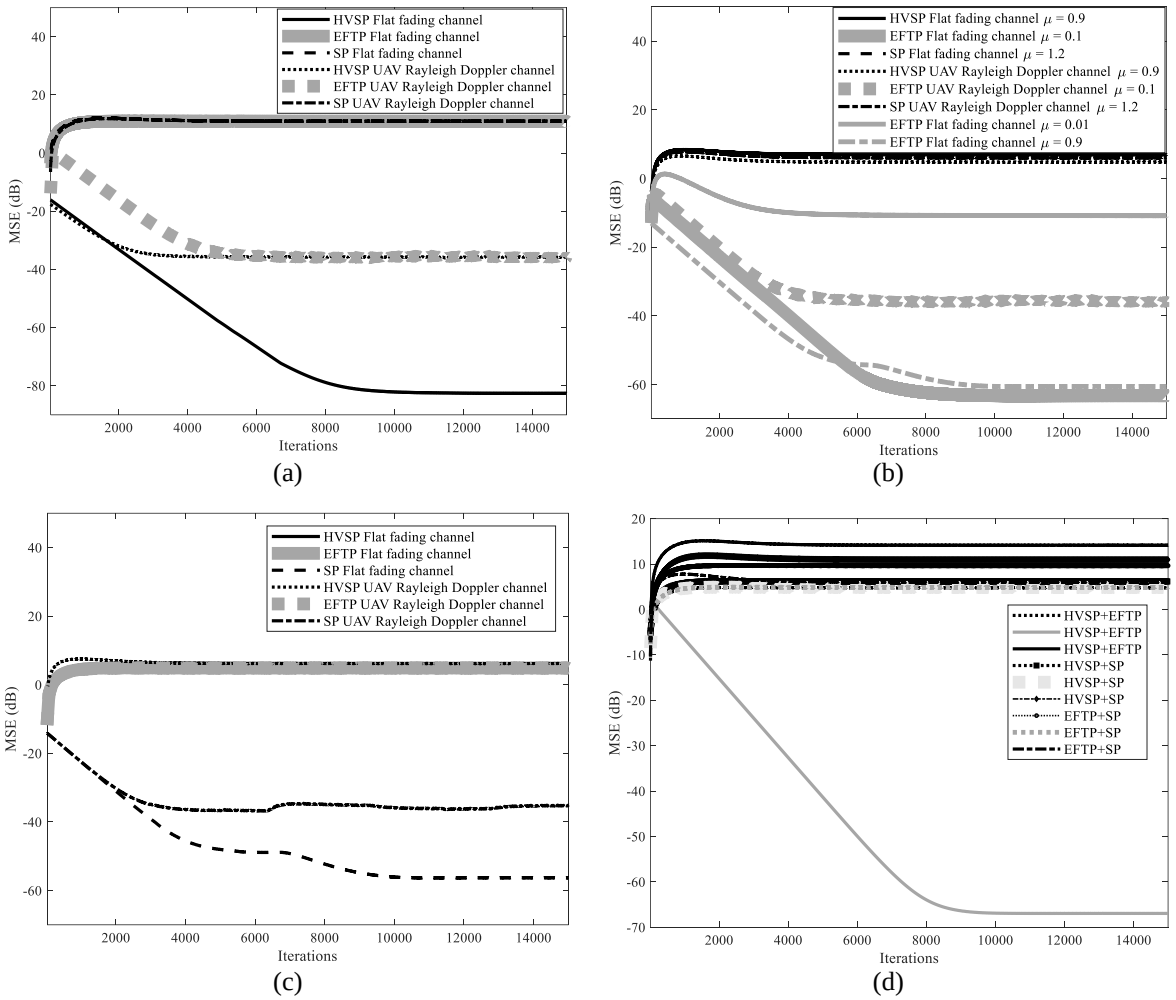

Figure 5. Convergence behavior of the MSE for various CV-VSS-NLMS algorithms in the proposed ANC system under two channel conditions; a flat fading channel and UAV Rayleigh Doppler channel: (a) communication link affected by HVSP noise, (b) communication link affected by EFTP noise, and (c) communication link affected by SP noise, and (d) communication links affected by simultaneous noise sources

Figure 5(b) illustrates the sensitivity analysis of the proposed CV-VSS-NLMS adaptive filter under the EFTP noise environment for different step-size values, particularly for μ = 0.9, 0.1 and 0.01. Based on the fact that the proposed algorithm employs a variable step-size adaptation mechanism, these values were selected to evaluate its performance under different adaptation rates. The obtained results show that the convergence behavior of the algorithm varies with changes in the step-size parameter, confirming the sensitivity of the proposed filter to this parameter.

As illustrated in Figure 5(d), the convergence of the MSE is analyzed for adaptive filters operating over communication links affected by simultaneous noise sources. Three noise combinations are considered: HVSP + EFTP, HVSP + SP, and EFTP + SP. It is evident from the Figure 5 that the adaptive filter achieves effective convergence only in the case where the filter is driven by the EFTP signal and the communication link is simultaneously affected by HVSP and EFTP noise sources. In this configuration, the filter exhibits the best MSE convergence performance, characterized by a faster convergence rate and a lower steady state MSE compared to the other cases.

Figures 6(a) to (c) present the cost function profiles at the output of the CV-VSS-NLMS algorithm under a communication link affected by HVSP noise, using adaptive filters driven by different noise types, HVSP, EFTP and SP, respectively. It should be clarified that the results presented in Figures 6 and 7 correspond to the flat fading channel scenario. According to the obtained results, it is evident that the cost function associated with the CV-VSS-NLMS filter driven by the noise corresponding to the one affecting the

communication link, particularly in the case of HVSP noise, exhibits the lowest energy compared to the others. This criterion thus makes it possible to identify and select the most suitable filter among the three, in order to provide the filtered signal with the best noise cancellation performance. Furthermore, as shown in Figures 7(a) to (c), the residual noise in the signal filtered by the appropriate CV-VSS-NLMS filter presents the lowest level, confirming the effectiveness of the filter selection strategy.

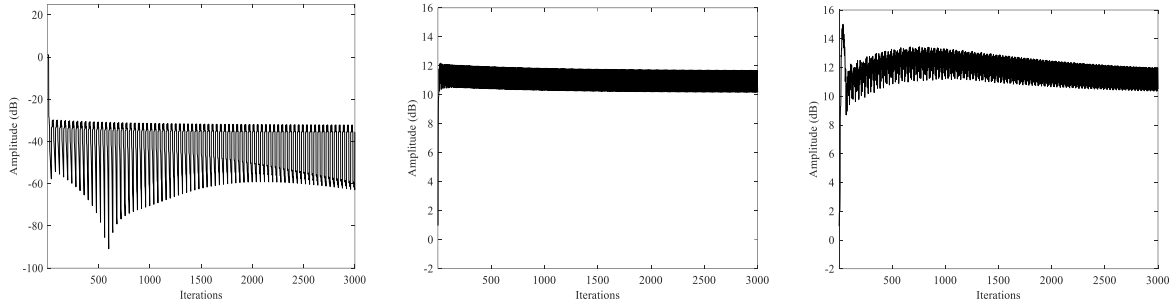

Figure 6. Cost function profile at the output of the CV-VSS-NLMS algorithm with the adaptive filter: (a) driven by HVSP noise and communication link affected by HVSP noise, (b) driven by EFTP noise and communication link affected by HVSP noise, and (c) driven by SP noise and communication link affected by HVSP noise

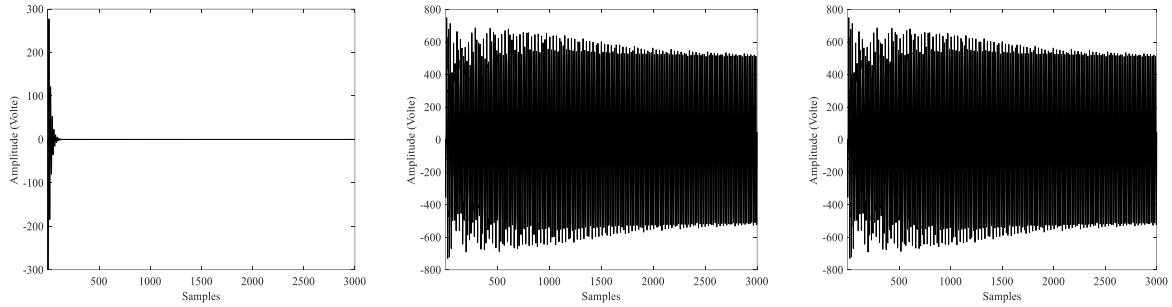

Figure 7. Residual interference in the communication link affected by HVSP noise and processed by the CV-VSS-NLMS algorithm: (a) driven by HVSP noise, (b) driven by EFTP noise, and (c) driven by SP noise.

Figures 8(a) to (c) respectively present the original communication signal, the communication signal corrupted by HVSP noise, and the de-noised signal at the output of the proposed system. It is clear that the de-noised signal closely matches the original signal, confirming the effectiveness of the proposed system.

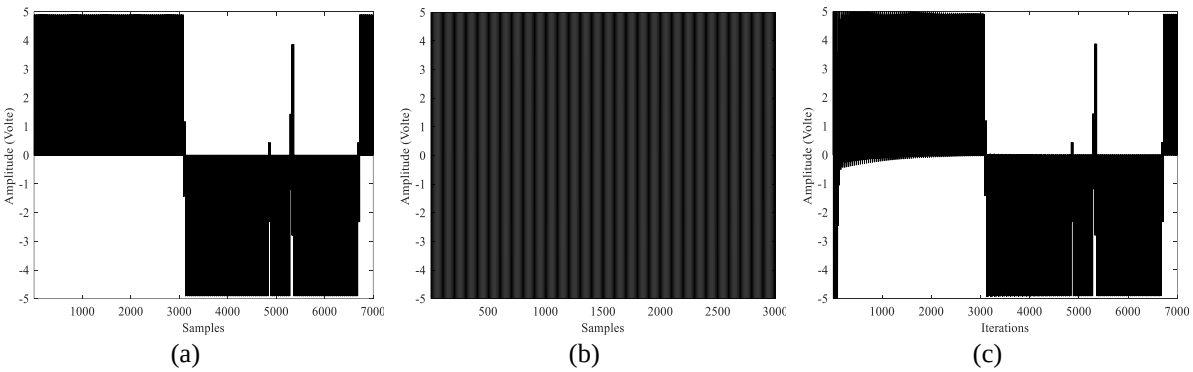

Figure 8. Communication link scenarios: (a) clean communication link, (b) noisy communication link, and (c) denoised communication link

Table 3 presents a comparison of the BER performance between the proposed noise suppression method and the existing method reported in [27] within the UAV-OFDM system, under three types of considered noises: HVSP, SP, and EFTP, all subjected to the same field strength amplitude of 500 V/m. The BER values for both the proposed and the existing methods were obtained using the image depicted in Figure 9.

Table 3. BER of the proposed noise suppression method

Corrupting noise	BER before de-noising (%)	BER after de-noising by the existing system [27] (%)	BER after de-noising by the proposed system (%)
HVSP noise	45.39	0.005597	0.000533
SP noise	45.39	0.004531	0.0032
EFTP noise	46.10	0.005597	0.0019

Figure 9. Original image

As shown in Table 3, the BER achieved using the proposed noise suppression method is significantly lower across all considered noise types, HVSP, SP, and EFTP, compared to the existing method proposed in [27], under a uniform field strength amplitude of 500 V/m. These results confirm the effectiveness of the proposed method in mitigating noise in the UAV-OFDM system. After applying the proposed noise suppression method, the BER is significantly reduced, approaching zero in all cases. Notably, the lowest BER is observed under HVSP noise conditions, indicating the most effective suppression performance among the three.

3.2. Computational complexity

This sub-section analyzes the computational complexity of the proposed algorithm and compares it with that of the conventional independent component analysis (ICA) method [27]. The evaluation is based on the number of arithmetic operations required, providing an objective measure of processing cost.

In the proposed algorithm, defined by (12)-(17), the total computational cost per filter is approximately $18N + 2L + 5$ multiplications and $14N + 2L$ additions. For the complete system, the overall complexity becomes $54N + 6L + 15$ multiplications and $42N + 6L$ additions, where N is the filter length and L is the smoothing window length.

In contrast, the ICA algorithm, described in [27], involves several computationally demanding steps, including de-meaning in (2), covariance estimation in (4), whitening in (3), iterative update in (5), weight adaptation in (6), normalization in (7) and (8), convergence testing in (9), and demixing in (11). The total complexity per iteration can be approximated as $2M^3 + 3M^2K + 3MK$ additions and $M^3 + 3M^2K + 3MK$ multiplications. Since the ICA algorithm must be executed separately two times for the real and imaginary parts of the complex OFDM signal. So, the total computational cost doubles, yielding approximately $4M^3 + 6M^2K + 6MK$ additions and $2M^3 + 6M^2K + 6MK$ multiplications, where M is the number of source signals and K the total number of samples.

For the purpose of comparison, we consider for instance the total number of samples used in [27], which is 3003136. By letting the parameters $L = 5$ and $N = 8$ in the above expressions, the proposed algorithm requires approximately 1.43×10^9 multiplications and 1.10×10^9 additions. Also, by letting the parameters $M = 2$ and the total number of iterations $I = 36$, the ICA algorithm requires approximately 3.89×10^9 multiplications and 3.89×10^9 additions. These numerical illustrations clearly demonstrate that the proposed algorithm achieves a significantly lower computational cost, being nearly three times more efficient than the conventional ICA method.

4. CONCLUSION

In this paper, we propose a novel approach for mitigating impulsive interference in OFDM-based UAV communication systems by developing an efficient CV-VSS-NLMS adaptive filtering algorithm. This approach extends existing LMS-based filtering principles to handle impulsive interference in UAV scenarios and integrates them within a well-designed single-antenna architecture. In contrast, real-valued VSS-LMS filters treat the real and imaginary parts separately, resulting in poorer MSE convergence for complex signals. Compared to conventional blind source separation techniques, the proposed method achieves better noise suppression. It exhibits fast MSE convergence, reaching steady states between -60 dB and -80 dB across the considered noise types, while maintaining a low residual noise level in the denoised signal. Moreover, it significantly reduces computational complexity and requires only 1.43×10^9 multiplications and 1.10×10^9 additions, compared to 3.89×10^9 multiplications and 3.89×10^9 additions required by the ICA approach. This reduction in the complexity corresponds to a gain of nearly a factor of three. This substantially lower computational complexity makes the proposed algorithm more practical for deployment in real-time constrained UAV applications. The superiority of the proposed approach is further confirmed by performance evaluations, which demonstrate notable efficiency in BER, specifically about 90% improvements under HVSP noise, 29% under SP noise, and 66% under EFTP noise. Furthermore, the proposed CV-VSS-NLMS algorithm provides a lightweight, efficient, and real-time solution for interference mitigation in UAV OFDM networks. As a future direction, the algorithm could be implemented on embedded hardware and tested through hardware-in-the-loop simulations or real UAV experiments.

FUNDING INFORMATION

Authors state no funding involved.

AUTHOR CONTRIBUTIONS STATEMENT

This journal uses the Contributor Roles Taxonomy (CRediT) to recognize individual author contributions, reduce authorship disputes, and facilitate collaboration.

Name of Author	C	M	So	Va	Fo	I	R	D	O	E	Vi	Su	P	Fu
Walid Lebbou		✓	✓	✓	✓	✓	✓	✓	✓		✓			
Laid Chergui	✓	✓	✓	✓	✓	✓	✓	✓	✓	✓	✓	✓	✓	
Saad Bouguezel			✓		✓					✓	✓			

C : **C**onceptualization
M : **M**ethodology
So : **So**ftware
Va : **Va**lidation
Fo : **Fo**rmal analysis
I : **I**nvestigation
R : **R**esources
D : **D**ata Curation
O : Writing - **O**riginal Draft
E : Writing - Review & **E**diting
Vi : **Vi**sualization
Su : **Su**pervision
P : **P**roject administration
Fu : **Fu**nding acquisition

CONFLICT OF INTEREST STATEMENT

Authors state no conflict of interest.

DATA AVAILABILITY

Authors state that data availability is not applicable to this paper as no new data were created or analyzed in this study.

REFERENCES

[1] S. J. R. and M. H. Saleh, "Online 3D path planning for Tri-copter drone using GWO-IBA algorithm," *TELKOMNIKA (Telecommunication Computing Electronics and Control)*, vol. 19, no. 4, p. 1334, Aug. 2021, doi: 10.12928/telkomnika.v19i4.18697.

[2] A. H. Wahyudi *et al.*, "Light weight dual polarized horn antenna for polarimetry C-band synthetic aperture radar sensor onboard UAV," *TELKOMNIKA (Telecommunication Computing Electronics and Control)*, vol. 22, no. 6, p. 1344, Dec. 2024, doi: 10.12928/telkomnika.v22i6.25718.

[3] C. Gupta and S. S. Yadav, "Deep Learning Based Channel Estimation for UAVs: A Modified U-Net Approach," *Advances in Electrical and Computer Engineering*, vol. 25, no. 1, pp. 61–70, 2025, doi: 10.4316/AECE.2025.01007.

[4] N. Khan, A. Ahmad, S. Ali, T. Jan, and I. Ullah, "IRS and UAV-relay assisted public safety networks for video transmission: optimizing UAVs deployment and resource allocation," *Telecommunication Systems*, vol. 86, no. 3, pp. 433–449, Jul. 2024, doi: 10.1007/s11235-024-01128-3.

[5] K. Surman and D. Lockey, "Unmanned aerial vehicles and pre-hospital emergency medicine," *Scandinavian Journal of Trauma,*

Resuscitation and Emergency Medicine, vol. 32, no. 1, p. 9, Jan. 2024, doi: 10.1186/s13049-024-01180-7.
[6] I. Umakoglu, M. Namdar, and A. Basgumus, "UAV-Assisted Cooperative NOMA System with the nth Best Relay Selection," *Advances in Electrical and Computer Engineering*, vol. 23, no. 3, pp. 39–46, 2023, doi: 10.4316/AECE.2023.03005.
[7] H. Yue, C. Guo, Q. Li, H. Chen, and Q. Zhang, "Power Allocation Optimization for Secure OFDM-NOMA Downlink Systems," *IEEE Open Journal of the Communications Society*, vol. 6, pp. 7555–7566, 2025, doi: 10.1109/OJCOMS.2025.3610253.
[8] F. D. L. Coutinho, S. S. Pereira, H. S. Silva, P. Georgieva, and A. S. R. Oliveira, "A Quantization-Aware DL-Based Channel Estimation Algorithm for OFDM Systems," *IEEE Access*, vol. 13, pp. 152608–152619, 2025, doi: 10.1109/ACCESS.2025.3604259.
[9] H. P. H. Shaw, M. Rowshan, and J. Yuan, "Improving OFDM Using Delay-Doppler Channel Estimation," *IEEE Open Journal of the Communications Society*, vol. 6, pp. 7184–7199, 2025, doi: 10.1109/OJCOMS.2025.3603197.
[10] M. Xu, C. T. Lam, Y. Liang, B. Ng, X. Yuan, and S. K. Im, "TDJSCC: Low Complexity and Bandwidth Efficient Deep Joint Source-Channel Coding With OFDM," *IEEE Access*, vol. 13, pp. 150244–150257, 2025, doi: 10.1109/ACCESS.2025.3602059.
[11] L. Chergui and S. Bouguezel, "A New Parametric DFT-Based OFDM Transceiver for Intrinsic Wireless Communication Encryption," *Advances in Electrical and Computer Engineering*, vol. 24, no. 1, pp. 15–22, 2024, doi: 10.4316/AECE.2024.01002.
[12] C. Qing, Z. Liu, W. Hu, Y. Zhang, X. Cai, and P. Du, "LoS Sensing-Based Channel Estimation in UAV-Assisted OFDM Systems," *IEEE Wireless Communications Letters*, vol. 13, no. 5, pp. 1320–1324, May 2024, doi: 10.1109/LWC.2024.3368652.
[13] S. Kumari, K. K. Srinivas, and P. Kumar, "Channel and Carrier Frequency Offset Equalization for OFDM Based UAV Communications Using Deep Learning," *IEEE Communications Letters*, vol. 25, no. 3, pp. 850–853, Mar. 2021, doi: 10.1109/LCOMM.2020.3036493.
[14] S. G. Kim, E. Lee, I. P. Hong, and J. G. Yook, "Review of Intentional Electromagnetic Interference on UAV Sensor Modules and Experimental Study," *Sensors*, vol. 22, no. 6, p. 2384, Mar. 2022, doi: 10.3390/s22062384.
[15] Z. Liu, Y. Li, and S. Shi, "Impulsive Noise Suppressing Method in Power Line Communication System Using Sparse Iterative Covariance Estimation," *Radio Science*, vol. 57, no. 4, Apr. 2022, doi: 10.1029/2022RS007424.
[16] L. Clavier, G. W. Peters, F. Septier, and I. Nevat, "Impulsive noise modeling and robust receiver design," *Eurasip Journal on Wireless Communications and Networking*, vol. 2021, no. 1, p. 13, Jan. 2021, doi: 10.1186/s13638-020-01868-1.
[17] Y. Zhao, Y. Li, S. Shi, and J. Yu, "Joint channel and impulse noise estimation based on compressed sensing and Kalman filter for OFDM system," *Eurasip Journal on Advances in Signal Processing*, vol. 2023, no. 1, p. 105, Oct. 2023, doi: 10.1186/s13634-023-01064-5.
[18] X. Feng, J. Wang, X. Kuai, M. Zhou, H. Sun, and J. Li, "Message Passing-Based Impulsive Noise Mitigation and Channel Estimation for Underwater Acoustic OFDM Communications," *IEEE Transactions on Vehicular Technology*, vol. 71, no. 1, pp. 611–625, Jan. 2022, doi: 10.1109/TVT.2021.3130061.
[19] L. Wu, "Mitigating impulsive noise for reliable UWA communication," *Nature Reviews Electrical Engineering*, vol. 2, no. 1, pp. 12–12, Jan. 2025, doi: 10.1038/s44287-024-00140-8.
[20] X. Li, Z. Han, H. Yu, L. Yan, and S. Han, "Deep Learning for OFDM Channel Estimation in Impulsive Noise Environments," *Wireless Personal Communications*, vol. 125, no. 3, pp. 2947–2964, Aug. 2022, doi: 10.1007/s11277-022-09693-z.
[21] K. Zhang, Y. Mao, S. Leng, and S. Fang, "Efficient anti-jamming strategies in multi-channel wireless networks," in *2013 Joint Conference of International Conference on Computational Problem-Solving and International High Speed Intelligent Communication Forum, ICCP and HSIC 2013*, IEEE, Oct. 2013, pp. 109–112, doi: 10.1109/ICCPS.2013.6893502.
[22] P. Chen, Y. Rong, S. Nordholm, Z. He, and A. J. Duncan, "Joint Channel Estimation and Impulsive Noise Mitigation in Underwater Acoustic OFDM Communication Systems," *IEEE Transactions on Wireless Communications*, vol. 16, no. 9, pp. 6165–6178, Sep. 2017, doi: 10.1109/TWC.2017.2720580.
[23] J. G. Wang *et al.*, "Suppressing Intentional Electromagnetic Interference (IEMI) in Wireless Communication System Using Complex Signal Spectrum Shifting Technique," in *2018 IEEE Symposium on Electromagnetic Compatibility, Signal Integrity and Power Integrity, EMC, SI and PI 2018*, IEEE, Jul. 2018, pp. 250–254, doi: 10.1109/EMCSI.2018.8495174.
[24] A. R. AlAjmi and M. A. Saed, "Microwave imaging with noise waveforms using FDTD time reversal method," *Microwave and Optical Technology Letters*, vol. 60, no. 5, pp. 1275–1280, May 2018, doi: 10.1002/mop.31148.
[25] R. I. Sokolov and R. R. Abdullin, "Restoration of Static JPEG Images and RGB Video Frames by Means of Nonlinear Filtering in Conditions of Gaussian and Non-Gaussian Noise," *Radio Science*, vol. 52, no. 11, pp. 1363–1373, Nov. 2017, doi: 10.1002/2017RS006392.
[26] Z. Yu, C. Wang, G. Cui, W. Wang, and Y. Zhang, "Phase noise estimation scheme based on linear interpolation for constant envelop OFDM system," in *2017 9th International Conference on Advanced Infocomm Technology (ICAIT)*, IEEE, Nov. 2017, pp. 279–284, doi: 10.1109/ICAIT.2017.8388930.
[27] Y. Jia, X. Tu, and W. Yan, "An UAV Wireless Communication Noise Suppression Method Based on OFDM Modulation and Demodulation," *Radio Science*, vol. 55, no. 2, Feb. 2020, doi: 10.1029/2019RS006959.
[28] S. Van Gerven and D. Van Compemolle, "Signal Separation by Symmetric Adaptive Decorrelation: Stability, Convergence, and Uniqueness," *IEEE Transactions on Signal Processing*, vol. 43, no. 7, pp. 1602–1612, Jul. 1995, doi: 10.1109/78.398721.
[29] R. Bendoumia and M. Djendi, "Two-channel variable-step-size forward-and-backward adaptive algorithms for acoustic noise reduction and speech enhancement," *Signal Processing*, vol. 108, pp. 226–244, Mar. 2015, doi: 10.1016/j.sigpro.2014.08.035.
[30] L. Chergui and S. Bouguezel, "Variable Step Size Pre-Whitening Transform Domain LMS Adaptive Noise Canceller," in *2019 International Conference on Advanced Systems and Emergent Technologies (IC_ASET)*, IEEE, Mar. 2019, pp. 327–331, doi: 10.1109/ASET.2019.8871012.
[31] E. M. Lobato, O. J. Tobias, and R. Seara, "Stochastic modeling of the transform-domain εLMS algorithm," *IEEE Transactions on Signal Processing*, vol. 56, no. 5, pp. 1840–1852, May 2008, doi: 10.1109/TSP.2007.909324.
[32] S. K. Nayak and M. J. Thomas, "Computation of EMI fields generated due to corona on high voltage over head power transmission lines," in *Proceedings of the International Conference on Electromagnetic Interference and Compatibility*, IEEE, 2002, pp. 15–19, doi: 10.1109/ICEMIC.2002.1006454.
[33] International Electrotechnical Commission, "Electromagnetic compatibility (EMC) - Part 4-4: Testing and measurement techniques - Electrical fast transient/burst immunity test," 2012.
[34] International Electrotechnical Commission (IEC), "Electromagnetic compatibility (EMC). Part 4-5, Testing and measurement techniques--surge immunity test," p. 155, 2017.
[35] V. Vahidi and E. Saberinia, "OFDM for payload communications of UAS: Channel estimation and ICI mitigation," *IET Communications*, vol. 11, no. 15, pp. 2350–2356, Oct. 2017, doi: 10.1049/iet-com.2017.0358.
[36] Y. Yapici and A. Ö. Yilmaz, "An analysis of the bidirectional LMS algorithm over fast-fading channels," *IEEE Transactions on Communications*, vol. 60, no. 7, pp. 1759–1764, Jul. 2012, doi: 10.1109/TCOMM.2012.050812.110116.

BIOGRAPHIES OF AUTHORS

Walid Lebbou received the Engineer degree in Electronics, and Master's degree from Badji Mokhtar-Annaba University, (June, 2009), (June, 2017) respectively, and currently he is Ph.D. student at Abbes Laghrour - Khenchela University Department of Electrical Engineering. He is also affiliated as a Researcher member (since March 2022)- SATIT research laboratory. He is currently a Senior Engineer and Head of Industrial Control Department, Mines and Metallurgy Research Unit, Research Centre in Industrial Technologies -CRTI- Algeria, His current research interests include communication engineering, computer engineering and automotive systems. He can be contacted at email: lebbou.walid@univ-khenchela.dz.

Laid Chergui received the Engineering degree in Electronics (Communication Engineering) from Badji Mokhtar University, Annaba, Algeria, in 2002, the Master's. degree in Electronics (Communication) from Ferhat Abbas University, Setif, in 2006, and the Ph.D. degree in Electronics from the same university in 2017, with a dissertation on "Speech Denoising Using Methods Based on Discrete Transforms." From 2012 to 2017, he was a lecturer in the Department of Industrial Engineering at Abbes Laghrour University, Khenchela, where he is now a Professor of Electronics in the Department of Electrical Engineering. He teaches undergraduate and graduate courses and is an active member of the SATIT research laboratory. As a research project leader, he supervises research in wireless signal processing, adaptive filtering, and embedded systems. His research interests include adaptive filtering, image processing, secure communication systems, and wireless signal processing. He can be contacted at email: chergui_laid@univ-khenchela.dz.

Saad Bouguezel received the Engineering degree in Electronics (Communication Engineering) from Setif 1 University Ferhat ABBAS, Setif, Algeria, in 1993, the Masters' degree in Electronics (Industrial Control) from Batna University, Batna, Algeria, in 1998, and the Ph.D. degree in Electrical Engineering from Concordia University, Montreal, QC, Canada, in 2004. From November 2004 to June 2006, he was a Postdoctoral Fellow in the Center for Signal Processing and Communications, Department of Electrical and Computer Engineering, Concordia University, where he was a research and teaching assistant from March 2002 to October 2004. From 1998 to February 2002, he was a lecturer within the Department of Electrical Engineering, Laghouat University, Laghouat, Algeria. In 2006, he joined the Department of Electronics at Setif 1 University Ferhat Abbas, Algeria, where he has been a Full Professor since 2012. His research interests include discrete transforms and their fast algorithms, techniques for signal and image processing, data compression, encryption, and digital watermarking. He also works on OFDM systems, biometric technologies such as fingerprint and face recognition, as well as artificial intelligence. He can be contacted at email: sbouguezel@univ-setif.dz.